Equal-spin triplet *p*-wave pairing in Nb/Ni proximity effect bilayers

W. J. Lu,[1] Y. K. Bang,[2] and K. Char[1,*]

[1]*Center for Strongly Correlated Materials Research, Department of Physics and Astronomy, Seoul National University, Seoul 151-742, Korea*

[2]*Department of Physics, Chonnam National University, Kwangju 500-757, Korea*

(Received 1 February 2010; published 22 April 2010)

Motivated by recent measurement of the anomalous subgap structure observed in the tunneling density of states (DOS) of superconductor/ferromagnet (S/F) proximity effect bilayers, we propose a model that accounts for this anomalous structure. Instead of using Usadel equation, we construct full Eilenberger equations suited for our Nb/Ni bilayers junction geometry allowing both singlet and triplet pairing correlations. Theoretical calculations of the DOS provide good qualitative and quantitative agreement with experimental data only when we allow *equal-spin triplet p-wave pairing correlation*. Our results strongly suggest the presence of equal-spin triplet *p*-wave pairing correlation, induced by an inhomogeneous magnetization in F region, in Nb/Ni bilayers.

DOI: 10.1103/PhysRevB.81.144514 PACS number(s): 74.45.+c, 73.23.−b, 74.50.+r

When a superconductor is placed in contact with a nonsuperconductor, near the interface the properties of both materials change due to the proximity effect. Remarkably, in the case of the superconductor/ferromagnet (S/F) proximity effect, dramatically different phenomena arise that are not present in either material alone. For example, on the F side of the interface the superconducting pair wave function decays in an oscillatory manner, leading to a pair density wave. These oscillations arise because the Cooper pairs, in the presence of an exchange field, acquire a finite momentum $q=2h/v_F$, where h is the exchange energy and v_F is the Fermi velocity.[1] The resulting modulated superconducting state is similar to the "Fulde-Ferrell-Larkin-Ovchinnikov" (FFLO) state in bulk materials.[2,3] This predicted oscillatory character of the pair wave function is now amply confirmed qualitatively by the observation of oscillations in the transition temperature of SF bilayers[4–6] and oscillation of the critical current in SFS Josephson π junctions,[7,8] both as a function of the thickness of the F layer.

Even more striking are predictions of induced triplet ($S=1$) pairing and an associated long-range proximity effect (when $S_z=\pm 1$). Conventionally, this triplet component would require an odd parity (e.g., *p*-wave) orbital pair wave function. However, as is well known, any finite-orbital angular-momentum pairing is strongly suppressed by elastic scattering. By this reasoning, triplet pairing can only occur in the clean limit.[9] Interestingly, there is another theoretical possibility that permits triplet pairing even in the dirty limit. If the superconductor adopts so-called odd-frequency (as opposed to the conventional even-frequency) pairing, the required antisymmetry of the pair wave function is preserved even for *s*-wave, triplet pairing. Such unconventional odd-frequency pairing, which was first proposed by Berezinskii[10] as a hypothetical state of superfluid ^{3}He, has been recently studied in Refs. 11–15 employing the Usadel theory in the dirty limit.

The possibility of such novel pairing states in the context of the superconductor/ferromagnet proximity effect with a conventional *s*-wave singlet superconductor has understandably drawn great attention. Definitive experimental evidence for these possible triplet states is lacking, although recent experimental observation by Keizer *et al.*[16] of a long-range Josephson supercurrent in SFS proximity structures where the F materials was the half-metallic ferromagnet CrO_2 is certainly suggestive of triplet ($S_z=\pm 1$) pairing in the F layer. These results have also been recently treated theoretically.[17] Evidence for triplet pairing on the S side of an SF bilayer—the so-called inverse proximity effect—was recently reported by Xia *et al.*[18] Still, experimental results that are sensitive to the specific symmetries of the pair wave function (frequency, orbital, and spin) are lacking. In this paper, we argue that recent anomalous spectroscopic structure in the tunneling density of states (DOS) of the F layer in Nb/Ni bilayers observed by one of us can be understood as a result of equal-spin triplet pairing induced by spatial variations in the magnetization of the F layer.

Superconducting tunneling DOS measurements[19] provide spectral information about the superconducting order parameter. As noted above, very recently, one of us reported an anomalous subgap structure in the tunneling DOS of the F side of Nb/Ni proximity bilayers,[20] which is also shown in Fig. 4(b). The unusual subgap structure cannot be explained by the "standard" Usadel equation in the dirty limit. In order to understand the behavior of two types of gaps in magnetic field, samples were measured in a perpendicular magnetic field, below H_{c2}(Nb). We plot the measured DOS of the $d_F=1.5$ nm sample in Fig. 1(a) for $H=0-3000$ Oe in 500 Oe increments. To isolate the outer gap, we measured the $d_F=1.0$ nm curve (it contains essentially no inner-gap structure) as a template. By properly scaling this template curve, we can then subtract that from the total DOS. The scale factor is adjusted such that the inner-gap curve is as featureless as possible at $\pm\Delta$. Mathematically, we can write this procedure as

$$N_{ig}(V,H)-1=[N(V,H)-1]-S(d_F)[N_t(V,H)-1], \quad (1)$$

where N_{ig} is the inner-gap DOS, N is the total DOS, N_t is the template DOS, and $S(d_F)$ is the scale factor. Figure 1(b) shows the difference in behavior between the outer gap and inner gap in a magnetic field. Comparing the shapes of the outer-gap and inner-gap curves as a function of field, we note that the peaks of the outer-gap curves become much lower

 ©2010 The American Physical Society

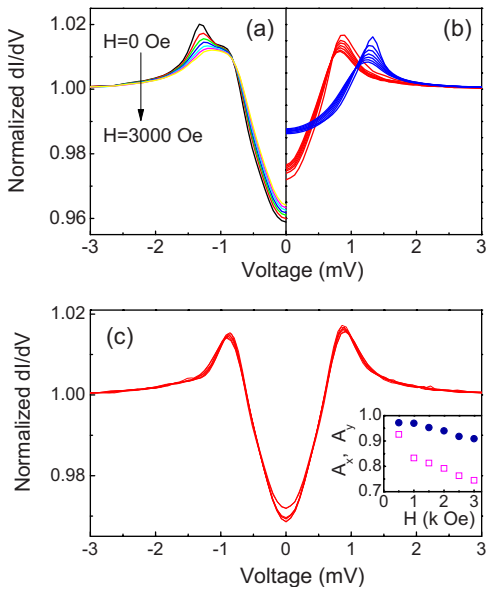

FIG. 1. (Color online) (a) Normalized conductances of $d_F = 1.5$ nm sample in a perpendicular magnetic field $H = 0, 500, \ldots, 3000$ Oe. (b) The same data, split into outer-gap (blue) and inner-gap (red) contributions. The $d_F = 1.0$ nm curve was measured at the same fields and each of theses curves was used as a template for that field. (c) Scaled inner-gap contribution to the DOS, using Eq. (2). For each magnetic field, the curve is stretched in the x and y directions until it is the same size as the $H = 0$ curve. The inset shows the scale factors A_x (circles) and A_y (squares).

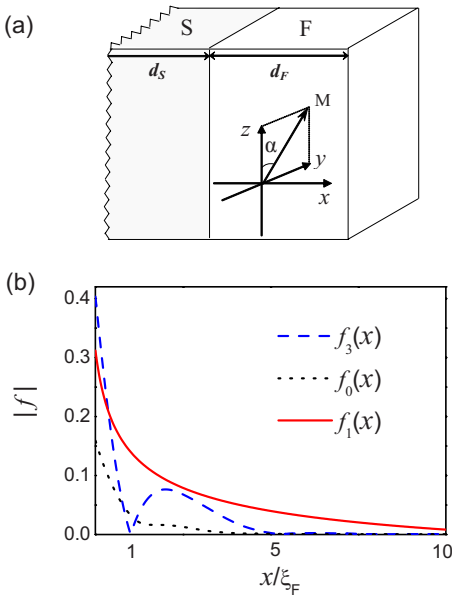

FIG. 2. (Color online) (a) Schematic illustration of S/F bilayer structure. The exchange field rotates in the F layer in the y-z plane and makes an angle α between M and the z axis. Here α varies linearly with x, i.e., $\alpha = Qx$. (b) Spatial dependence of the pair amplitude $|f|$ in the F layer for the singlet (dashed, blue), $S_z = 0$ triplet (dotted, black), and $S_z = \pm 1$ triplet (solid, red) components. Here $\epsilon = 0$ and other parameters are same as those used in DOS calculation of Nb/Ni.

and broader as the field increases while the shape of the inner-gap curves appears to remain roughly constant, even as its height and width slightly shrink.

In order to compare the shapes of the curves more exactly, we can scale all of the inner-gap curves such that they are same height and width. The scaled curves obey the equation

$$N_s(V,H) - 1 = A_y^{-1}(H)\{N_o[A_x^{-1}(H)V,H] - 1\}, \qquad (2)$$

where N_s is the scaled curve, N_o is the original curve, $A_x(H)$ is the voltage scale factor, and $A_y(H)$ is the conductance scale factor. Figure 1(c) shows the scaled inner-gap curves for all measured magnetic fields and the related scale factors $A_x(H)$ and $A_y(H)$ are shown in the inset. All the curves collapse to a single curve almost exactly, which suggests that the shape of the inner-gap DOS is not affected by an applied magnetic field. Furthermore, the collapsed DOS curve in Fig. 1(c) has a V-like shape rather than the usual U-like shape, which reminds of a DOS with a gap node in momentum space. This clearly stimulates further research and serves as a motivation for employing more sophisticated models of a S/F interface, possibly including a local magnetization inhomogeneity in the F region.[14]

We consider the S/F structure shown in Fig. 2(a); it consists an in-plane rotating magnetization M in the F layer. For simplicity, we assume that the magnetization orientation varies linearly with x, i.e., $\alpha = Qx$, where α is the angle between M and the z axis and Q the pitch wave vector. Of course, a more realistic model of the inhomogeneous magnetic field at the interface would be much more complex—taking into account domain walls, spin-orbit coupling, and magnetic impurities—but this arrangement produces the simplest inhomogeneous micromagnetic model which can be theoretically calculated.

We start with the Eilenberger equation[1,21] for the anomalous Green's function $\hat{f}(\omega, \mathbf{R}, \mathbf{v})$ generalized to the full pairing symmetry, including the spin singlet and triplet pairings

$$\hat{f}(\omega,\mathbf{R},\mathbf{v}) = \begin{pmatrix} f_{\uparrow\downarrow} & f_{\uparrow\uparrow} \\ f_{\downarrow\downarrow} & f_{\downarrow\uparrow} \end{pmatrix} = \begin{pmatrix} f_+ & f_{\uparrow\uparrow} \\ f_{\downarrow\downarrow} & f_- \end{pmatrix}. \qquad (3)$$

In the above equation, ω is the Matsubara frequency, $\mathbf{R}$ is the center of mass coordinate of the paired particles, and $\mathbf{v}$ is the Fermi velocity of one of the paired particles. The Eilenberger equation for $f_\pm(\omega,\mathbf{R},\mathbf{v})$, including the exchange field and spin-orbit scattering in addition to the ordinary nonmagnetic impurity scattering, takes the form[1]

$$\left(\tilde{\omega} \pm ih - \frac{1}{2}\mathbf{v}\frac{\partial}{\partial \mathbf{R}}\right) f_\pm(\omega,\mathbf{R},\mathbf{v}) = \tilde{\Delta}_\pm(\omega,\mathbf{R},\mathbf{v}), \qquad (4)$$

where $\tilde{\Delta}_\pm(\omega,\mathbf{R},\mathbf{v}) = \Delta + \frac{1}{2\tau_1}\int \frac{d\Omega'}{4\pi} f_\pm(\omega,\mathbf{R},\mathbf{v}') + \frac{3}{2\tau_{so}}\int \frac{d\Omega'}{4\pi} f_\mp(\omega,\mathbf{R},\mathbf{v}')\sin^2(\theta-\theta')$ and $\tilde{\omega} = \omega + \frac{1}{2\tau_1} + \frac{1}{\tau_{so}}$ (τ_1 is elastic scattering time and τ_{so} is spin-orbit scattering time). Assuming a simple one-dimensional geometry of the tunneling junction [see Fig. 2(a)], all quantities depend only on the coordinate x and the function $f_\pm(\omega,x,\mathbf{v})$ is expanded only up to the second order using the Legendre polynomials $f_\pm(\omega,x,\mathbf{v}) = f_\pm^0(\omega,x) + f_\pm^1(\omega,x)\cos\theta$, where θ is the angle between $\mathbf{n}$ (direction of the Fermi velocity $\mathbf{v} = \mathbf{n}v_F$) and x

axis. With this expansion and integrations of Eq. (4) with $\int d\theta$ and $\int d\theta \cos\theta$, we obtain the standard results as follows:

$$(\omega \pm ih) f_{\pm}^{0} - \frac{v_F}{6}\frac{\partial}{\partial x} f_{\pm}^{1} = \Delta - \frac{1}{\tau_{so}}(f_{\pm}^{0} - f_{\mp}^{0}), \tag{5}$$

$$\left(\omega \pm ih + \frac{1}{2\tau_1} + \frac{1}{\tau_{so}}\right) f_{\pm}^{1} = \frac{v_F}{2}\frac{\partial}{\partial x} f_{\pm}^{0}. \tag{6}$$

The usual Usadel approximation takes an approximation of $(\omega \pm ih + \frac{1}{2\tau_1} + \frac{1}{\tau_{so}}) \rightarrow (\frac{1}{2\tau_1})$, which is applicable in the dirty limit ($1/\tau_1 \gg \omega$, h, and $1/\tau_{so}$). But in reality this condition may not be satisfied in the pure ferromagnet metal. Here we keep the above full information. Treating $f_{\pm}^{0}$ and $f_{\pm}^{1}$ on an equal footing, we obtain the following equations for the F layer (note that superconducting order parameter Δ vanishes in the ferromagnet):

$$\frac{1}{2}D\frac{\partial^2}{\partial x^2} f_{\pm}^{0} - (\omega \pm ih)\left(\omega \pm ih + \frac{1}{2\tau_t}\right) 2\tau_t f_{\pm}^{0} = \frac{2\tau_t}{\tau_{so}}\left(\omega \pm ih + \frac{1}{2\tau_t}\right)[f_{\pm}^{0} - f_{\mp}^{0}], \tag{7}$$

$$\frac{1}{2}D\frac{\partial^2}{\partial x^2} f_{\pm}^{1} - (\omega \pm ih)\left(\omega \pm ih + \frac{1}{2\tau_t}\right) 2\tau_t f_{\pm}^{1} = \frac{\tau_t}{\tau_{so}} v_F \frac{\partial}{\partial x}[f_{\pm}^{0} - f_{\mp}^{0}], \tag{8}$$

where $\frac{1}{2\tau_t} = \frac{1}{2\tau_1} + \frac{1}{\tau_{so}}$ and $D = \frac{1}{3}\tau_t v_F^2$. After adding and subtracting the above four equations (upper and lower signs), we can obtain following four equations containing the four combinations of $f_{\pm}^{0}$ and $f_{\pm}^{1}$:

$$\left\{\frac{1}{2}D\frac{\partial^2}{\partial x^2} - \left[\left(\omega + \frac{2}{\tau_{so}}\right)(1 + \omega\cdot 2\tau_t) - 2\tau_t \cdot h^2\right]\right\} f_{sing,even}^{s} - ih[1 + 4\omega\cdot\tau_t] f_{trip,odd}^{s} = 0, \tag{9}$$

$$\left\{\frac{1}{2}D\frac{\partial^2}{\partial x^2} - [\omega(1 + \omega\cdot 2\tau_t) - 2\tau_t \cdot h^2]\right\} f_{trip,odd}^{s} - ih\left[1 + 4\tau_t\cdot\left(\omega + \frac{1}{\tau_{so}}\right)\right] f_{sing,even}^{s} = 0, \tag{10}$$

$$\left\{\frac{1}{2}D\frac{\partial^2}{\partial x^2} - [\omega(1 + \omega\cdot 2\tau_t) - 2\tau_t \cdot h^2]\right\} f_{trip,even}^{p} - ih[1 + 4\omega\cdot\tau_t] f_{sing,odd}^{p} = 0, \tag{11}$$

$$\left\{\frac{1}{2}D\frac{\partial^2}{\partial x^2} - \left[\left(\omega + \frac{2}{\tau_{so}}\right)(1 + \omega\cdot 2\tau_t) - 2\tau_t \cdot h^2\right]\right\} f_{sing,odd}^{p} - ih\left[1 + 4\tau_t\cdot\left(\omega + \frac{1}{\tau_{so}}\right)\right] f_{trip,even}^{p} = 0, \tag{12}$$

where $f_{sing,even}^{s} = [f_{+}^{0} - f_{-}^{0}]$, $f_{trip,odd}^{s} = [f_{+}^{0} + f_{-}^{0}]$, $f_{trip,even}^{p} = [f_{+}^{1} + f_{-}^{1}]$ and $f_{sing,odd}^{p} = [f_{+}^{1} - f_{-}^{1}]$. These four coupled equations are equivalent to the matrix Eilenberger equations, recently solved by Eschrig and Löfwander[17] for the S/F (half-metal) junction proximity effects. In this paper, our purpose is not to examine all possible theoretical solutions for the S/F junction but to find out solutions to best understand our experimental data. Omitting numerous trials, we briefly summarize our final and successful process as follows.

As a first trial, we combine only Eqs. (9) and (10), which allows the *s*-wave odd-frequency triplet ($f_{trip,odd}^{s}$) and is similar to the work of Bergeret *et al.*[14] These equations can be generalized as a matrix form to include the equal spin triplet components $f_{\uparrow\uparrow}$ and $f_{\downarrow\downarrow}$ using Eq. (3) $\hat{f} = \hat{f}_{sing} + \hat{f}_{trip}$; with $\hat{f}_{sing} = f_3\sigma_3$ and $\hat{f}_{trip} = f_0\sigma_0 + f_1\sigma_1$ as follows:

$$-iD\partial_x^2\hat{f} + 2\tilde{\epsilon}\hat{f} + \{\hat{V}, \tilde{h}\cdot\hat{f}\} + i4/\tau_{so}(1 - i\epsilon\cdot 2\tau_t)\cdot\hat{f}_{sing}^{s} = 0, \tag{13}$$

where we use the energy ϵ to replace Matsubara frequency $i\omega$, $\tilde{\epsilon} = \epsilon(1 - i2\tau_t\epsilon) - i2\tau_t h^2$, and $\{\ldots\}$ is the anticommutator. The term $\tilde{h}\cdot\hat{f}$ means $\Sigma_{i=0,1,3}\tilde{h}_i f_i\sigma_i$ with $\tilde{h}_{0,1} = h(1 - i4\tau_t\epsilon)$, and $\tilde{h}_3 = h(1 - i4\tau_t\epsilon + \frac{4\tau_t}{\tau_{so}})$. The matrix $\hat{V} = \hat{\sigma}_3\cos(Qx) + \hat{\sigma}_2\sin(Qx)$ ($\hat{\sigma}_i$ are the Pauli matrices) is introduced to simulate an inhomogeneous exchange field $h(x)$. In reality, the origins and detailed forms of the inhomogeneous exchange field can be many but the main physical effect is the same, i.e., to convert the $S_z = 0$ triplet component to the $S_z = \pm 1$ equal spin-triplet component and vice versa by rotating the spin quantization axis.[13,14] On the other hand, the equation for the S layer is as follows: $-iD\partial_x^2\hat{f} + 2\epsilon\hat{f} - 2\Delta\hat{\sigma}_3 = 0$. Additionally the proper boundary conditions are: $\hat{f}^{F}|_{x=0+} = \hat{f}^{S}|_{x=0-}$ and $\xi_N\gamma\partial_x\hat{f}^{F}|_{x=0+} = \xi_S\partial_x\hat{f}^{S}|_{x=0-}$, where $\xi_S = \sqrt{D_S/2\Delta}$, $\xi_N = \sqrt{D_F/2\Delta}$, and $\gamma = \rho_S\xi_S/\rho_F\xi_N$ [$D_{S(F)}$ and $\rho_{S(F)}$ are the diffusion constants and the resistivities of S(F) layer]. Note that these boundary conditions reflect simple reflection and transmission at the interface with no magnetic effects.

As clearly seen from Eqs. (9) and (10), the singlet component f_{sing} and $S_z = 0$ triplet component $f_{trip,S_z=0}$ are mixed by a homogeneous exchange field $\tilde{h}$ and therefore both components decay inside of the F layer with the same length scale $k_h^{-1} = \sqrt{D/\tilde{h}}$, as shown in Fig. 2(b). But the equal spin-triplet component $f_{trip,S_z=\pm 1}$ is generated by the inhomogeneous exchange field $\hat{V}$ from the $S_z = 0$ triplet component $f_{trip,S_z=0}$ and once created it can penetrate in the length scale $k_Q^{-1} = (\sqrt{k_\epsilon^2 + Q^2})^{-1}$, where $k_\epsilon^2 = -2i\epsilon/D$.[14] In the limit of small $Q \ll k_\epsilon, k_h$ (a slow rotating magnetization), the induced equal spin-triplet pairing can penetrate into F layer over long distances, which is the so-called long-range triplet component.[13,14] When Q is close to k_h, like the singlet pairing, the equal spin triplet pairing can become the short-range component.

Choosing an Ansatz for the solution $\hat{f}$ of Eq. (13) in the form $\hat{f} = f_{sing}\hat{\sigma}_3 + f_{trip,S_z=0}\hat{\sigma}_0 + if_{trip,S_z=\pm 1}\hat{\sigma}_1$, we indeed obtain the solution where the equal spin-triplet component $f_{trip,S_z=\pm 1}$ is an odd function of frequency, $\mathrm{Re}\, f_{trip,S_z=\pm 1}(\omega) = -\mathrm{Re}\, f_{trip,S_z=\pm 1}(-\omega)$, as discussed by Ref. 14. The DOS curve can be calculated by using $N(x,\epsilon)$

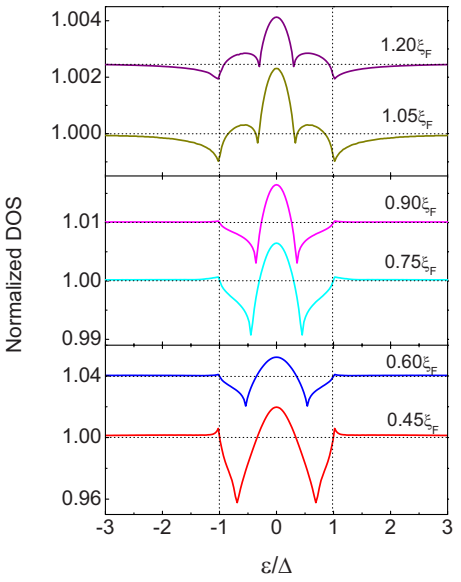

FIG. 3. (Color online) The calculated DOS for S/F bilayers with various thickness of F layers using odd-frequency pair model. A conductance peak at zero bias is clearly seen.

$=N_0\,\mathrm{Re}\{\sqrt{1-f(x,\epsilon)f^{\dagger}(x,\epsilon)}\}$ where N_0 is the local DOS in the normal state. We find the DOS curve for the odd-frequency s-wave triplet component shows a conductance peak at zero bias due to the node at zero frequency in odd-frequency superconductor, as shown in Fig. 3, which is consistent with other previous theoretical reports.[11,12] However, this result is in marked contrast to the strong anomalous subgap structure observed in our measured DOS of Nb/Ni bilayer; in all our measured DOS any signature of peak structure at zero energy is at best at the noise level.

This situation has motivated us to consider the possible realization of even-frequency p-wave triplet pairing. If the F layer is not too dirty (pure Ni layers may fall between the clean and dirty limits), it was shown to be possible.[17] To allow $f^{p}_{trip,even}$, we combine Eqs. (9) and (11) and its matrix generalization has the same form as Eq. (13). But now, the $\hat{f}_{trip}$ matrix contains even- and odd-frequency components together. To emphasize the even-frequency p-wave triplet (which is indeed a dominant solution with our parameters), we take a different Ansatz $\hat{f}=f_{sing}\hat{\sigma}_3+f_{trip,S_z=0}\hat{\sigma}_0+f_{trip,S_z=\pm1}\hat{\sigma}_1$. Without having "$i$" in front of $f_{trip,S_z=\pm1}\hat{\sigma}_1$, the symmetry of $f_{trip,S_z=\pm1}$ is indeed determined by Eq. (13) to be $\mathrm{Re}\, f_{trip,S_z=\pm1}(\omega)=\mathrm{Re}\, f_{trip,S_z=\pm1}(-\omega)$. Being an even-frequency triplet, the $f_{trip,S_z=\pm1}$ wave function should have a p-wave orbital symmetry. This orbital degree of freedom ($\cos\theta$ in its lowest order) was stripped off in the derivation of Eqs. (5) and (6) and now we need to put it back for the calculation of DOS such as $f_{trip,S_z=\pm1}(x,\epsilon,\theta)=f_{trip,S_z=\pm1}\cos\theta$. Within the above formulation, we can calculate, by numerical methods, the local DOS for the equal-spin p-wave triplet component $f_{trip,S_z=\pm1}$ from $N(x,\epsilon)=N_0\int_0^{\pi/2}d\theta\,\mathrm{Re}\{\sqrt{1-f_{trip,S_z=\pm1}(x,\epsilon,\theta)f^{\dagger}_{trip,S_z=\pm1}(x,\epsilon,\theta)}\}$. We calculate the local DOS at zero temperature and compare the calculated results with our previous experimental data of Nb/Ni tunnel junctions.

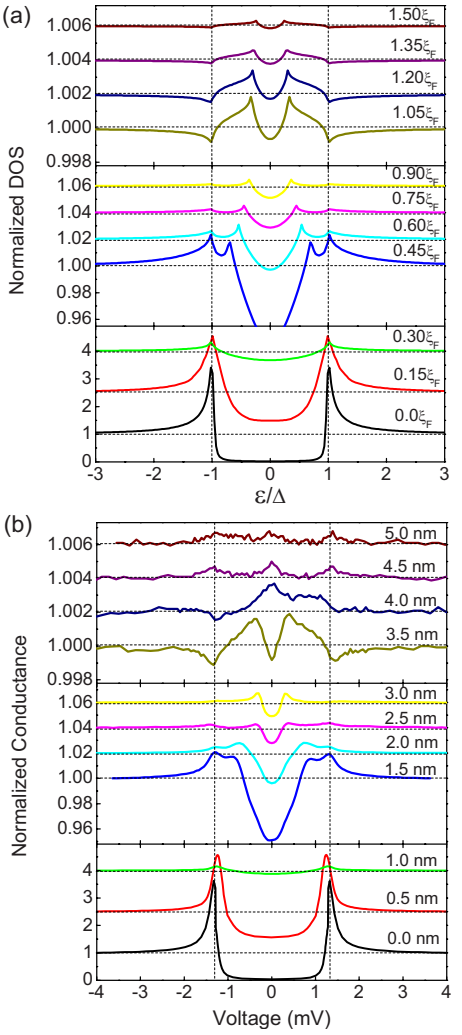

FIG. 4. (Color online) (a) The calculated DOS as a function of ϵ for S/F bilayers with various thickness of F layers (ξ_F=3.3 nm). From the bottom to the top plot the vertical scale is successively amplified and the curves are shifted for clarity. (b) Normalized conductances of Nb/Ni junctions measured at 0.28 K for various Ni thickness indicated inside (see Ref. 20 for details).

In order to fit the measured DOS data of Nb/Ni junctions [see Fig. 4(b)], we calculate the DOS using the reasonable fixed parameters (close to the previously established values in Refs. 5 and 20) Δ=1.3 meV, h=40Δ, ξ_S=7 nm, ξ_N=21 nm, γ=0.4, and $1/\tau_1$=4Δ ($1/\tau_1 \gg \Delta$ for the dirty limit) and the fitting parameters τ_{so} and Q. Our calculation indicates that we can qualitatively and quantitatively fit the overall feature size of outer gap at $\pm\Delta$ as a function of thickness, d_F, by the addition of a finite τ_{so} term. If we add the finite Q parameter (a large value of $Q>\pi/2\xi_F$), the subgap structure can be produced, which cannot be explained by the "standard" Usadel equation.[20] In Fig. 4(a), we present the calculated DOS using parameters $1/\tau_{so}=15\Delta$, and $Q=2\pi/3\xi_F$(ξ_F=3.3 nm), which fit the measured DOS reasonably well especially when the thickness d_F is less than 4.0 nm. The d_F=0 curve has two clear BCS coherence peaks at $\epsilon=\pm\Delta$; above that, the feature size decreases with increasing thickness for the d_F/ξ_F=0.15 and 0.3, indicating the su-

perconductivity is strongly suppressed by the exchange field. For $d_F/\xi_F=0.45-0.90$, in addition to the general trend of decreasing feature size as a function d_F, we see a double peak structure of the DOS, with the interior peaks moving to lower energy as d_F increases. Our calculation indicates that the subgap results from the equal spin-triplet-pairing component. The decreasing width of the subgap with thickness d_F is reminiscent of the "minigap" phenomenon seen in S/N bilayers.[22] In S/N system, the tunneling DOS shows a superconducting gap whose width decreases on a length scale ξ_N. In our Nb/Ni system, the subgap width decreases on a length scale k_Q^{-1} which is determined by Q value. When $d_F/\xi_F>1$, the inverted DOS (the coherence peaks at $\pm\Delta$ are now minima) appears while the interior gap remains. The inverted DOS behavior is related to the "π state" with a negative sign of the singlet order parameter.[19] We note that the measured DOS of $d_F \geq 4.0$ nm is close to the limits of the measurement and becomes less reliable, especially in the region near zero bias,[20] which cannot be compared with our calculated DOS. We must point out that the peaks in measured DOS are much broader than those in our calculated DOS due to the lifetime broadening of quasiparticles at a finite temperature (0.28 K for our measurement).

Considering the virtually unchanged subgap in magnetic field and the good agreement between our model calculations and experimental measurements, we suggest the $S_z=\pm 1$ equal spin-triplet pairing plays an important role in the proximity effect in Nb/Ni bilayers. The reported giant proximity effect in the Al/Ni and Al/Ho systems may also be due to this equal spin-triplet pairing.[23] Generating p-wave pairing correlation due to broken symmetries is quite generic phenomena, for example, as observed in the noncentrosymmetric compounds.[24,25] On the other hand, in the case of Nb/CoFe, we have not observed any subgap features, nor the inversion of DOS;[26] the magnitude of s-wave singlet DOS was simply reduced as the CoFe thickness increased. The important remaining issue is what actual mechanism converts the $S_z=0$ triplet pairs to the $S_z=\pm 1$ triplet pairs. In our present theory, we considered the simplest model of helical magnetism in F layer. Even when more realistic model of inhomogeneous magnetization only at the interface was considered, overall qualitatively fitting of the data did not change much. Judging from our calculations above, we can presume that the actual equal-spin conversion mechanism prefers even-frequency component to odd-frequency component. In reality, the S/F interface as a "spin-active" interface is complex.[13,17] Further theoretical studies should be taken based on more sophisticated models of a S/F interface, possibly including a domain-wall structure, spin-orbit scattering, and local magnetic impurities.

In conclusion, we consider a theoretical model in which equal spin-triplet pairing is generated by an inhomogeneous magnetization and numerically calculate the DOS of Nb/Ni bilayers in two different models: s-wave odd frequency and p-wave even frequency. We find the calculated DOS compares well to our measurements in the case of p-wave even-frequency model. We suggest the possibility of p-wave equal spin-triplet correlations in Nb/Ni bilayers. We note that we made an *ad hoc* selection of equations out of the complete set of Eqs. (9)–(12) to calculate the even-frequency p-wave part. We do not know why the odd-frequency s-wave component is suppressed in our experiments which should coexist theoretically with the even-frequency p-wave component.[17] Further experimental and theoretical investigation should be invoked, especially on the mechanism of conversion to equal-spin triplet component. Considering that the observation of the FFLO state in bulk materials is still controversial despite intensive efforts of search for more than four decades and that the bulk triplet superconductivity [^{3}He,[27] UPt_3,[28] and Sr_2RuO_4 (Ref. 29)] is extremely rare compared to the abundant singlet superconductivity, the S/F systems can provide an alternate route to study the novel superconductivity phenomena.

ACKNOWLEDGMENTS

The authors appreciate the critical reading and the feedback by Paul SanGiorgio and Mac Beasley and acknowledge the support of BK21 Foundation of Korea and KOSEF through Accelerated Research Program (Grant No. R17-2008–33-01000-0) (W.J.L. and K.C.) and Grant No. KRF-2007-521-C00081 (Y.K.B.).

*kchar@phya.snu.ac.kr

[1] E. A. Demler, G. B. Arnold, and M. R. Beasley, Phys. Rev. B **55**, 15174 (1997).
[2] P. Fulde and R. A. Ferrell, Phys. Rev. **135**, A550 (1964).
[3] A. I. Larkin and Y. N. Ovchinnikov, Sov. Phys. JETP **20**, 762 (1965).
[4] J. S. Jiang, D. Davidović, D. H. Reich, and C. L. Chien, Phys. Rev. Lett. **74**, 314 (1995).
[5] J. Kim, J.-H. Kwon, K. Char, H. Doh, and H. Y. Choi, Phys. Rev. B **72**, 014518 (2005).
[6] V. Zdravkov, A. Sidorenko, G. Obermeier, S. Gsell, M. Schreck, C. Müller, S. Horn, R. Tidecks, and L. R. Tagirov, Phys. Rev. Lett. **97**, 057004 (2006).
[7] V. V. Ryazanov, V. A. Oboznov, A. Y. Rusanov, A. V. Veretennikov, A. A. Golubov, and J. Aarts, Phys. Rev. Lett. **86**, 2427 (2001).
[8] T. Kontos, M. Aprili, J. Lesueur, F. Genêt, B. Stephanidis, and R. Boursier, Phys. Rev. Lett. **89**, 137007 (2002).
[9] M. Eschrig, J. Kopu, J. C. Cuevas, and G. Schön, Phys. Rev. Lett. **90**, 137003 (2003).
[10] V. L. Berezinskii, JETP Lett. **20**, 287 (1974).
[11] Y. Tanaka and A. A. Golubov, Phys. Rev. Lett. **98**, 037003 (2007).
[12] A. F. Volkov and K. B. Efetov, Phys. Rev. B **78**, 024519 (2008).
[13] F. S. Bergeret, A. F. Volkov, and K. B. Efetov, Rev. Mod. Phys. **77**, 1321 (2005); A. I. Buzdin, *ibid.* **77**, 935 (2005).
[14] F. S. Bergeret, A. F. Volkov, and K. B. Efetov, Phys. Rev. Lett. **86**, 4096 (2001).

[15] T. Yokoyama, Y. Tanaka, and A. A. Golubov, Phys. Rev. B **75**, 134510 (2007).
[16] R. S. Keizer, S. T. B. Goennenwein, T. M. Klapwijk, G. Miao, G. Xiao, and A. Gupta, Nature (London) **439**, 825 (2006).
[17] M. Eschrig and T. Löfwander, Nat. Phys. **4**, 138 (2008).
[18] J. Xia, V. Shelukhin, M. Karpovski, A. Kapitulnik, and A. Palevski, Phys. Rev. Lett. **102**, 087004 (2009).
[19] T. Kontos, M. Aprili, J. Lesueur, and X. Grison, Phys. Rev. Lett. **86**, 304 (2001).
[20] P. SanGiorgio, S. Reymond, M. R. Beasley, J. H. Kwon, and K. Char, Phys. Rev. Lett. **100**, 237002 (2008).
[21] G. Eilenberger, Z. Phys. **214**, 195 (1968).
[22] S. Guéron, H. Pothier, N. O. Birge, D. Esteve, and M. H. Devoret, Phys. Rev. Lett. **77**, 3025 (1996).
[23] V. T. Petrashov, I. A. Sosnin, I. Cox, A. Parsons, and C. Troadec, Phys. Rev. Lett. **83**, 3281 (1999); I. Sosnin, H. Cho, V. T. Petrashov, and A. F. Volkov, *ibid.* **96**, 157002 (2006).
[24] M. Sigrist, in *Lectures on the Physics of Strongly Correlated Systems XIII: Thirteenth Training Course*, AIP Conf. Proc., No. 1162 (AIP, New York, 2009), p. 55.
[25] V. N. Krivoruchko and V. Yu. Tarenkov, Phys. Rev. B **75**, 214508 (2007); **78**, 054522 (2008).
[26] S. Reymond, P. SanGiorgio, M. R. Beasley, J. Kim, T. Kim, and K. Char, Phys. Rev. B **73**, 054505 (2006).
[27] A. J. Leggett, Rev. Mod. Phys. **47**, 331 (1975).
[28] H. Tou, Y. Kitaoka, K. Asayama, N. Kimura, Y. Ōnuki, E. Yamamoto, and K. Maezawa, Phys. Rev. Lett. **77**, 1374 (1996).
[29] K. Ishida, H. Mukuda, Y. Kitaoka, K. Asayama, Z. Q. Mao, Y. Mori, and Y. Maeno, Nature (London) **396**, 658 (1998).